Heterogeneous Acrylic Resins with Bicontinuous Nanodomains as Low-Modulus Flexible Adhesives

Jong-Ho Back, Ji-Soo Kim, Youngdo Kim, and Hyun-Joong Kim*

Adhesives play a critical role in the assembly of electronic devices, particularly as devices become more diverse in form factors. Flexible displays require highly transparent and rapidly recoverable adhesives with a certain stiffness. In this study, novel structured adhesives are developed that incorporate bicontinuous nanodomains to fabricate flexible adhesives with low moduli. This structure is obtained via polymerization-induced microphase separation using a macro chain transfer agent (CTA). Phase separation is characterized using small-angle X-ray scattering, transmission electron microscopy, and dynamic mechanical analysis. By optimizing the length of the macro CTA, an adhesive with both hard and soft nanodomains is produced, resulting in exceptional flexibility (strain recovery = 93%) and minimal modulus (maximum stress/applied strain = 7 kPa), which overperforms traditional adhesives. The optimized adhesive exhibits excellent resilience under extensive strain, as well as strong adhesion and transparency. Furthermore, dynamic folding tests demonstrate the exceptional stability of the adhesive under various temperature and humidity conditions, which is attributed to its unique structure. In summary, the distinct bicontinuous phase structure confers excellent transparency, flexibility, and reduced stiffness to the adhesive, rendering it well-suited for commercial foldable displays and suggesting potential applications in stretchable displays and wearable electronics.

1. Introduction

Recently, electronics have transformed from rigid to flexible, foldable, and stretchable.[1–4] These electronics contain various
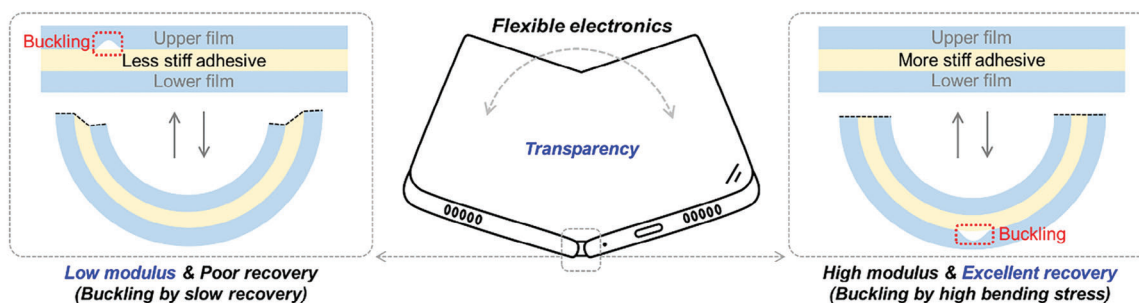
J.-H. Back, J.-S. Kim, H.-J. Kim
Program in Environmental Materials Science
Department of Agriculture
Forestry and Bioresources
Seoul National University
Seoul 08826, Republic of Korea
E-mail: hjokim@snu.ac.kr
J.-H. Back, H.-J. Kim
Research Institute of Agriculture and Life Sciences
College of Agriculture and Life Sciences
Seoul National University
Seoul 08826, Republic of Korea
Y. Kim
Samsung Display Co. Ltd.
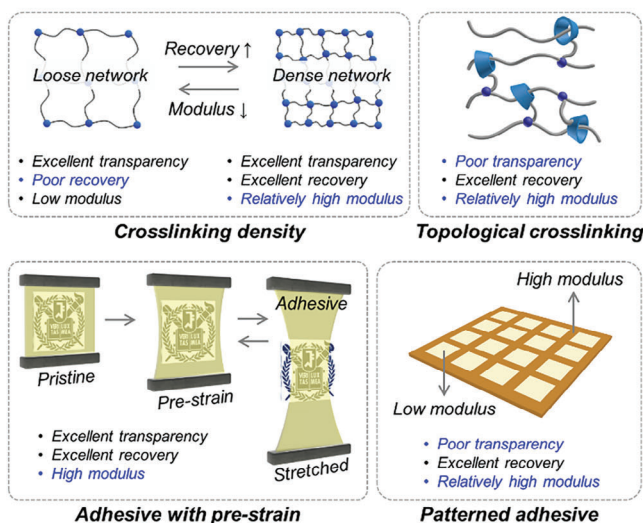Cheonan 31086, Republic of Korea

components, such as flexible substrates, device layers, and adhesives. Adhesives are crucial for joining flexible electronics; however, with the advancements in electronics technology, they must also perform other functions, such as conducting electricity,[5–7] wrapping around materials,[8] and transferring circuits.[9,10] For flexible displays, adhesives must meet three primary criteria: be transparent, recover quickly, and have a certain stiffness (**Figure 1a**). First, the transparency of the adhesive is critically linked to power consumption, as adhesives with poor transparency can significantly reduce display brightness.[11,12] Second, the adhesive must quickly return to its original shape when unfolded to prevent buckling when opened.[13–15] Third, the adhesive modulus should be sufficiently low to avoid buckling during folding. Making the adhesive softer reduces the stress when folding and creates a stress-neutral plane in rigid substrates rather than the soft adhesive, which results in significant improvement in folding stability.[16–19]

Numerous studies have focused on fabricating adhesives for flexible displays, which can be grouped into four primary strategies (Figure 1b; Table S1, Supporting Information). First, our group demonstrated that the crosslinking density is strongly related to the recovery and modulus of the adhesives.[20,21] Adhesives with loose crosslinking had a low modulus but did not recover well, whereas densely crosslinked adhesives exhibited the opposite behavior. Second, Lee et al.[14,15] created adhesives using a preexisting strain to achieve excellent recovery properties. However, despite being transparent, these adhesives were extremely stiff because of their densely crosslinked structures. Third, we developed a method called topological crosslinking using cyclodextrin that resulted in adhesives with excellent flexibility and recovery.[22,23] However, these adhesives were not sufficiently transparent for display use, and their moduli must be increased for better recovery. Finally, we focused on creating heterogeneous adhesives with both high- and low-modulus areas in one adhesive.[24,25] These different modulus zones reduced the bending stress while enabling good recovery.[24] In addition, the continuous phase of the hard domain offered excellent adhesive recovery properties.[25] However, it was difficult to further reduce the modulus because of the lightly crosslinked structure of the softer areas, and there was

ADVANCED
SCIENCE NEWS
www.advancedsciencenews.com

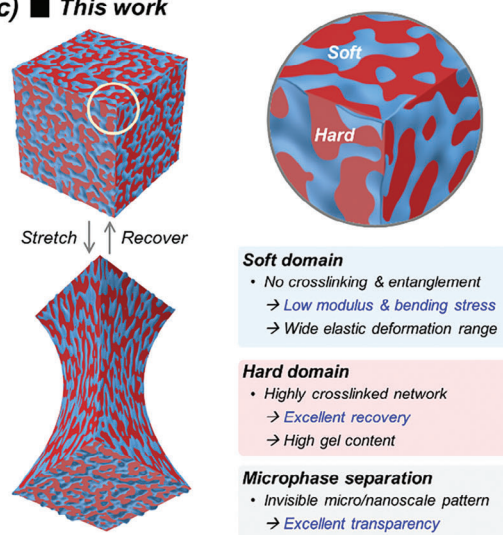NANO · MICRO
small
www.small-journal.com

Figure 1. a) Schematic illustration of transparent adhesives for flexible electronics. b) Common strategies for the preparation of flexible adhesives. c) Schemes of heterogeneous adhesives with a nano-scaled bicontinuous phase.

an issue with visible patterns due to the large scale of patterns. Therefore, there is a high demand for submicron-scale heterogeneous adhesives containing crosslinking-free soft domains and continuous phases comprising hard domains.

A promising way to fabricate nanoscale heterogeneous polymers is by separating the phases of block copolymers. One method that has attracted attention is polymerization-induced self-assembly (PISA) because it requires fewer steps to produce the nanoscale bicontinuous phase of block copolymers.[26–28] However, PISA can only be used in solvent-based processes, which conflicts with the current initiative to avoid solvents in fabricating adhesives.[29–32] A better option for preparing a nanoscale bicontinuous phase is polymerization-induced phase separation (PIPS), which does not require solvents.[33] Traditionally, PIPS has been extensively used to induce macro-scaled phase separation in epoxy systems, enhancing their ductility and toughness.[34] Based on PIPS, Seo and Hillmyer developed polymerization-induced microphase separation (PIMS), allowing for more precise morphological control at smaller scales.[35] PIMS creates a nano-scaled continuous phase consisting of hard and crosslinking-free soft domains,[36,37] which is ideal for developing low-modulus flexible adhesives with excellent transparency.

In this study, heterogeneous adhesives with nanoscale bicontinuous phases were fabricated as low-modulus flexible adhesives (Figure 1c). The soft domains rendered the adhesive less stiff, whereas the hard domains enabled it to recover quickly when stretched. Ensuring the domain size was on the submicron scale assisted in creating a transparent adhesive. We employed a light-curing-based PIMS to create a nanoscale bicontinuous phase, and the adhesive composition was optimized to ensure that it recovered quickly while having a certain stiffness. The phase separation behavior was observed using small-angle X-ray scattering (SAXS), transmission electron microscopy (TEM), and viscoelasticity tests. Mechanical analyses, including tensile, recovery/relaxation, and cyclic tensile tests, were conducted to determine the optimal composition. Finally, the adhesive strength, transparency, and folding stability of the optimal adhesives were characterized.

2. Results and Discussion

2.1. Design Strategy

Since its first development in 2012,[35] PIMS has been widely used to fabricate bicontinuous nanodomains for nanoporous

Table 1. Schemes for the a) formation of the nanoscale bicontinuous phase and b) composition of the heterogeneous adhesive with bicontinuous nanodomains. [TPO] was set as 0.5, and "DP" represents the degree of polymerization of PBA in the macro CTA.
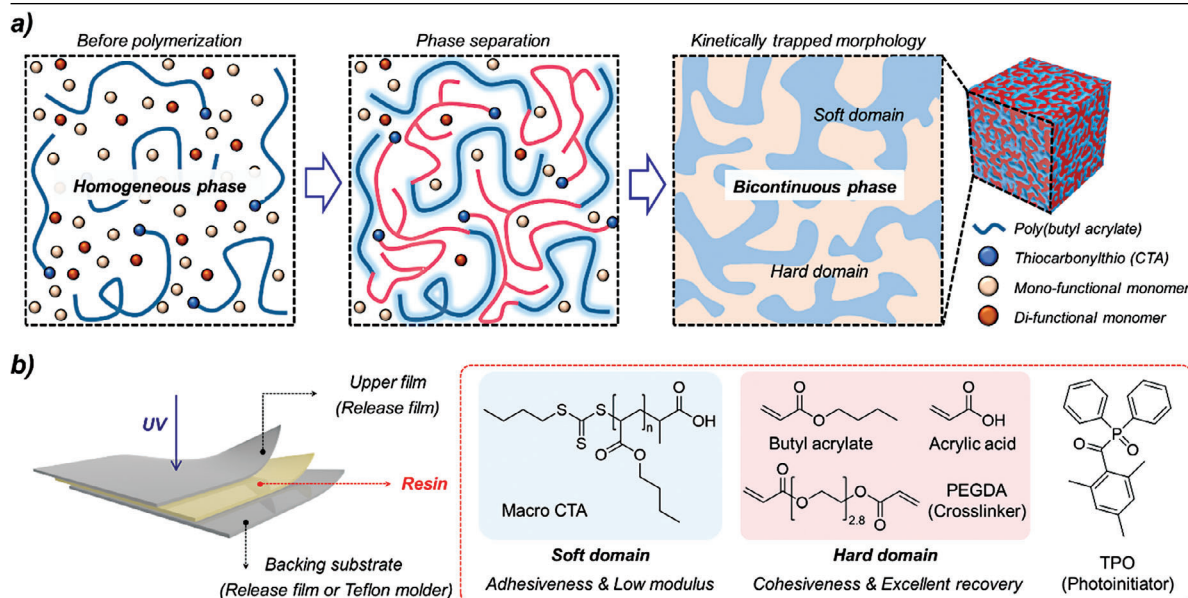
Entry		[Macro CTA]	[Butyl acrylate]	[Acrylic acid]	[PEGDA]
Macro CTA	DP = 80	0.5	55	5	0.5
	DP = 100	0.4			
	DP = 200	0.2			
	DP = 400	0.08			
	DP = 1000	0.04			
Oligomer (DP = 100, no CTA)		0.4	55	5	0.5
w/o Macro CTA (no soft domain)		–	95	5	0.5

materials[35,38] and polymer electrolyte membranes.[39–42] Notably, light-curing-based PIMS has been developed to produce 3D printable materials,[43–45] offering considerably quicker polymerization than the traditional azobisisobutyronitrile-based polymerization reaction. We anticipate its superiority in the preparation of solvent-free and light-curable adhesives.

The primary constituents of PIMS include a macro chain transfer agent (CTA), radical initiator, and blend of monomers (**Table 1**, Scheme a).[36,37] Initially, the macro CTA is soluble within the monomer blend, and the second block begins growing from its end. As polymerization progresses, the resulting polymer becomes incompatible with the remaining unreacted monomer blend, resulting in phase separation. At this point, the separated phase is kinetically trapped by the crosslinked network of the second block, ultimately yielding a nanoscale bicontinuous phase.

In this study, we prepared heterogeneous adhesives with two distinct nanoscale phases: soft and hard domains (Table 1, Scheme b). For the soft domain, we used a hydrophobic poly(butyl acrylate) (PBA)-based macro CTA. The hard domain comprised a blend of butyl acrylate (BA), acrylic acid (AA), and poly(ethylene glycol) diacrylate (PEGDA; crosslinker, $M_n = 250$ g mol^{-1}), thus offering relatively high hydrophilicity. Polymeriza-

tion was initiated using diphenyl(2,4,6-trimethylbenzoyl) phosphine oxide (TPO), a commonly used photoinitiator.

As previously reported, the molecular weight of the macro CTA has a significant impact on both the phase separation behavior and mechanical characteristics of the resultant polymers.[45] Therefore, we synthesized various macro CTAs with different molecular weights (Table S2, Supporting Information). The compositions of the soft and hard domains are listed in Table 1, and the macro CTA content was determined using preliminary testing (Table S3, Supporting Information). The molar ratio of the monomers in the final polymer was consistently maintained at [BA]: [AA] = 95:5, the standard composition for acrylic adhesives.[46,47] In addition to heterogeneous adhesives with macro CTAs, we prepared homogeneous adhesives without macro CTAs and heterogeneous adhesives containing PBA oligomers and lacking CTAs for control experiments.

2.2. Phase Separation

To confirm the successful formation of the nanoscale bicontinuous phase, we characterized the domain size and morphology using SAXS and TEM (**Figure 2a,b**). Adhesives lacking macro CTAs

■ *Phase separation*
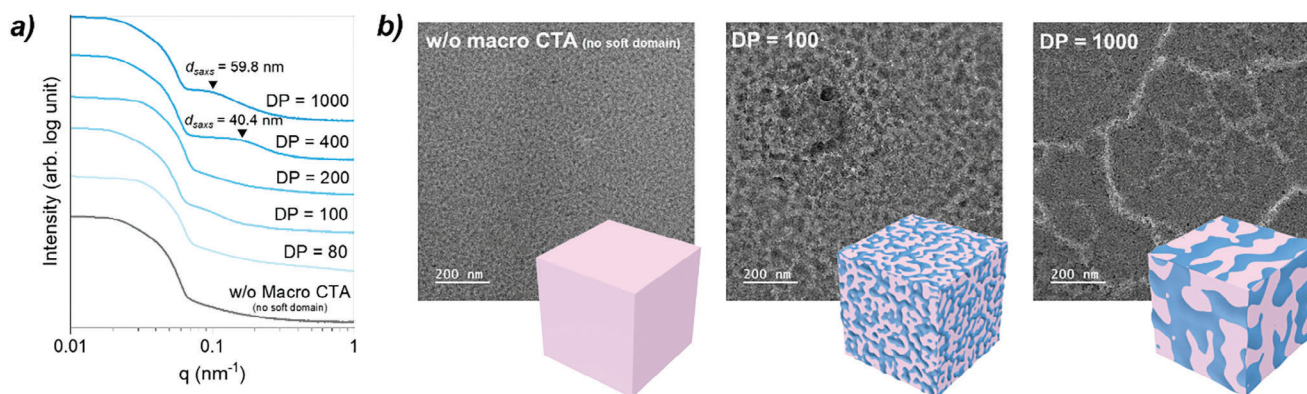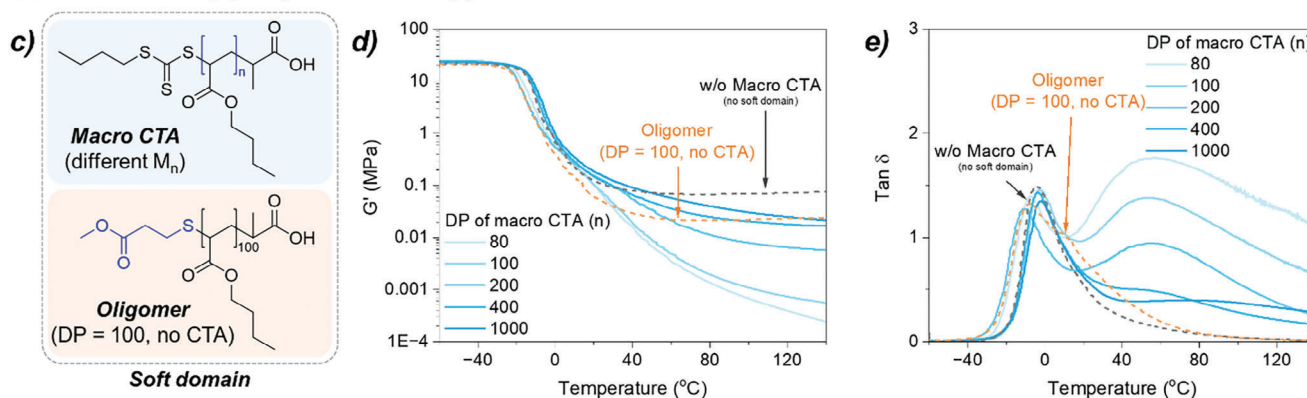

■ *Viscoelasticity (temperature sweep)*

Figure 2. a) SAXS and (b) TEM results of the homogeneous adhesive (gray line, without macro CTA) and heterogeneous adhesive with different DPs of macro CTAs. c) Chemical structures of the macro CTAs and oligomers of soft domains in the heterogeneous adhesives. Temperature-dependent (d) storage modulus and (e) tan δ results of the homogeneous and heterogeneous adhesives.

or those containing low-molecular-weight macro CTAs displayed no observable peaks in the SAXS results, suggesting that the prepared adhesives were homogeneous rather than heterogeneous. The size of the bicontinuous nanodomains increased with the increasing degree of polymerization (DP) of the macro CTAs,[45] as demonstrated in the TEM images and shifts in peaks within the SAXS data. Moreover, the width of the peak surpassed that of a typical bicontinuous polymer obtained via PIMS, which could be attributed to the large domain size distribution.[48] In the instances of heterogeneous adhesives prepared using a macro CTA with a DP of 100, phase separation was not apparent in SAXS; however, TEM images revealed nanoscale bicontinuous phase separation (Figure S1, Supporting Information). This could be attributed to the weak segregation strengths of the soft and hard domains.

Phase separation of the prepared adhesive was further confirmed based on its viscoelastic properties (Figure 2c–e). The homogeneous adhesive that lacked the macro CTA exhibited a singular tan δ peak, while the heterogeneous adhesives with a macro CTA or oligomer displayed peak splitting. The tan δ peak originating from the soft domain of the PBA block was absent in the heterogeneous adhesives, a phenomenon commonly encountered in PIMS-based polymers containing PBA blocks.[43–45] Instead, peak splitting in the tan δ curve was evident in the hard

domain of P(BA-*sat*-AA-*sat*-PEGDA), which is typically observed in bicontinuous polymers containing a high content of macro CTAs.[44,45] The amplitude of the tan δ peaks that were separated in the higher temperature region ($\approx$60 °C) decreased with an increase in the DP of the macro CTA. This could be attributed to the enhancement of the melt flow resistance of the PBA block adjacent to the hard domain. The heterogeneous adhesive with the PBA oligomer displayed less peak splitting, probably due to the weak interaction and segregation strength between the PBA and P(BA-*sat*-AA-*sat*-PEGDA) domains.

2.3. Physical Properties

The tensile properties of the prepared adhesives were assessed to confirm that the bicontinuous phase provided flexible adhesives with low stiffness. As shown in **Figure 3a**, the elastic moduli of the heterogeneous adhesives were significantly lower than those of the homogeneous adhesive without the macro CTA (217 kPa). Because the soft domain within the patterned adhesives induced lower stress levels than the hard domain, the overall stress experienced by the patterned adhesives was diminished in comparison to that experienced by the homogeneous adhesives.[24] Furthermore, CTA addition during the crosslinking

■ **Tensile test**
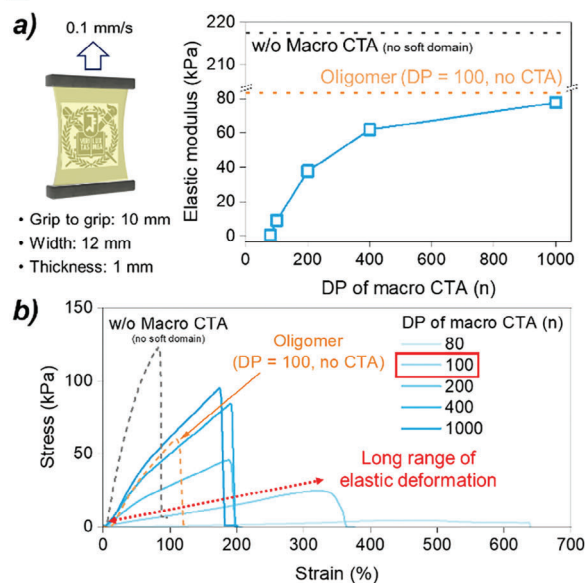
■ **Strain recovery/Stress relaxation**
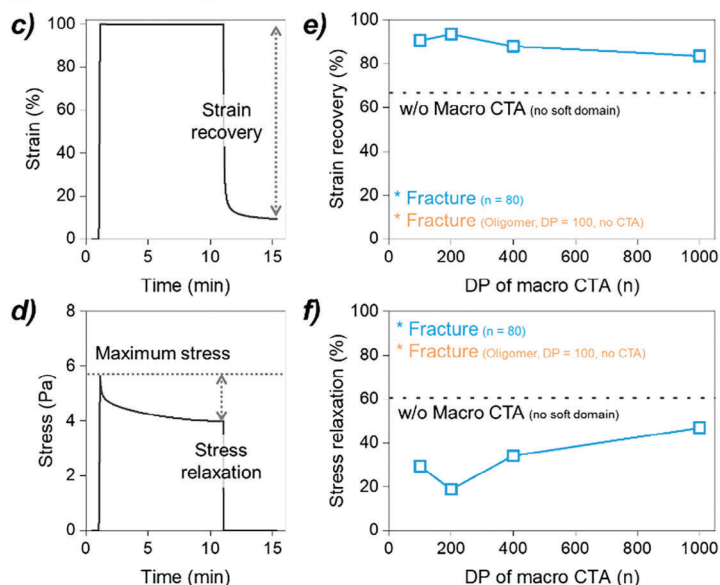
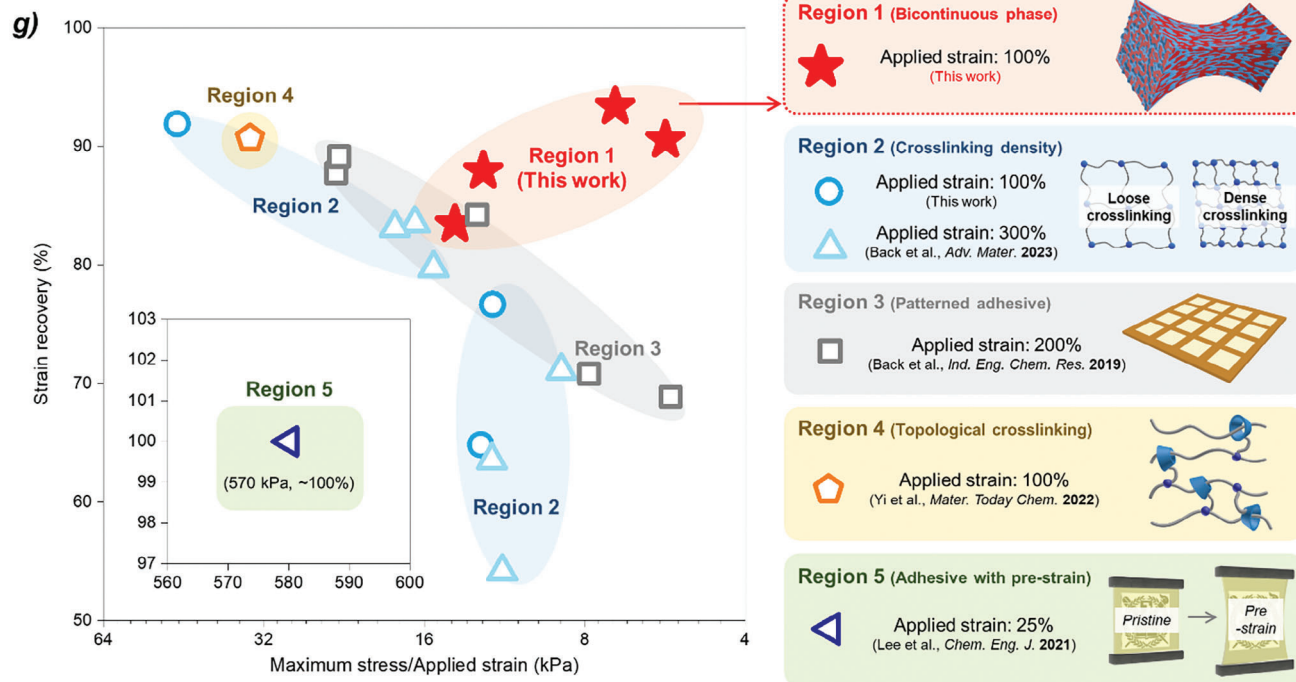■ **Strain recovery vs maximum stress/applied strain**

Figure 3. a) Tensile test scheme, elastic modulus, and (b) strain–stress curves of the prepared adhesives. Representative curves of (c) strain–time and (d) stress–time for the strain recovery/stress relaxation test. e) Strain recovery and (f) stress relaxation results with different DP values for the macro CTA. g) Maximum strain recovery stress/applied strain for the adhesives in this study and in the literature.[14,23,24,53]

process formed branching structures instead of 3D networks,[49] thereby reducing the crosslinking density in the hard domain (Figure S2, Supporting Information). Particularly, when the DP of the PBA block was held constant at 100, the adhesive containing the macro CTA exhibited an exceptionally low modulus (9.18 kPa) in contrast to the PBA oligomer lacking the CTA (83.2 kPa). This result could be attributed to the higher crystallinity and crosslinking density of the adhesive containing the

PBA oligomers (Figure S3, Supporting Information). In addition, when the DP was 100, the heterogeneous adhesive exhibited an extensive range of elastic deformations (>300%) without strain hardening (Figure 3b; Figure S3, Supporting Information). This finding may be ascribed to two factors: the bicontinuous phase and low crosslinking density. First, the co-continuous phases comprising crosslinked and soft domains enabled an even distribution of stress, potentially enhancing the elongation at

**ADVANCED
SCIENCE NEWS**

www.advancedsciencenews.com

**NANO · MICRO
small**

www.small-journal.com

break.[45,50] Second, a loosely crosslinked network could facilitate elastic deformation over a wide range without strain hardening and bond rupture.[51] When the DP exceeded 100, the molecular weight between the crosslinking points (M_c) of the heterogeneous adhesives considerably decreased (<50 kg mol^{-1}) owing to the entanglement of the PBA block (Figure S2, Supporting Information). Thus, the heterogeneous adhesive containing the macro CTA with entanglement-free short PBA blocks (entanglement molecular weight of PBA = 28 kg mol^{-1})[52] offered a low crosslinking density (DP = 100, M_c = 166 kg mol^{-1}).

Flexible adhesives must return to their original shape quickly without plastic deformation, which is strongly related to their recovery and relaxation properties. To assess strain recovery and stress relaxation, we applied 100% strain for 10 min and then removed the stress for a 5-min recovery period (Figure 3c,d). Adhesives prepared with insufficient gel content (macro CTA, DP = 80) or limited elongation (PBA oligomer without CTA) broke during testing. The homogeneous adhesive lacking the macro CTA endured the test conditions but showed only partial strain recovery (66.6%) and significant stress relaxation (60.3%) owing to its plastic deformation (Figure 3e,f). However, the heterogeneous adhesives with the macro CTA demonstrated better strain recovery and less stress relaxation than the homogeneous adhesive, indicating that they were more elastic. Particularly, the optimized adhesive (macro CTA, DP = 100) demonstrated significant strain recovery (90.6%) and reduced stress relaxation (29.2%).

For flexible electronics, adhesives must recover quickly and not be overly stiff, which can be evaluated using the plot between strain recovery and maximum stress per applied strain (Figure 3g). Employing a pre-straining technique resulted in notable strain recovery but yielded adhesives that were too stiff (Region 5).[14] Utilizing topological crosslinking accelerated adhesive recovery, but the stiffness of the material remained excessively high (Region 4).[23] Adjusting the crosslinking density, a commonly employed method for flexible adhesives, yielded various adhesive options. However, the strain recovery significantly decreased as the maximum stress per applied strain was reduced (Region 2).[53] Introducing heterogeneous adhesives with millimeter-scale patterns improved the strain recovery at a lower maximum stress per applied strain (<10 kPa), although the overall strain recovery remained below 71% (Region 3).[24] In our study, we developed bicontinuous phase-based adhesives (Region 1) with exceptional strain recovery (>90.6%) and an extremely low maximum stress per applied strain (<7.02 kPa). These findings indicated that the fabrication of a bicontinuous phase was the most effective approach for producing flexible adhesives with minimal stiffness.

To further investigate the flexibility of the prepared adhesives, we conducted cyclic tensile tests on both the heterogeneous and homogeneous adhesives. The heterogeneous adhesive, which contained a PBA oligomer (DP = 100, no CTA), and the homogeneous adhesive, which contained a high concentration of crosslinker (PEGDA, 0.5), failed when subjected to a 300% strain. However, reducing the crosslinker content to 0.1 enabled the resulting homogeneous adhesive to withstand a strain of 300%, although with a significant residual strain exceeding 50% (**Figure 4**b; Figure S3, Supporting Information). Notably, the heterogeneous adhesive incorporating the macro CTA (DP = 100) exhibited exceptional flexibility (Figure 4a) with minimal resid-

ual strain (<20%) and stress (<9 kPa). From the cyclic test, resilience can be determined by analyzing the area under the stress-strain curve during both the loading and unloading processes (Figure S5, Supporting Information). Resilience is defined as the ability to undergo reversible deformation without energy dissipation. Therefore, highly resilient adhesives exhibit minimal differences in cyclic curves across multiple cycles. For instance, a hydrogel adhesive used for wound sealing patches should exhibit high resilience to endure the dynamic movements of the body, with a resilience of ≈70%.[54] However, as shown in Figure 4c, the initial loading–unloading cycle demonstrated excellent resilience for the heterogeneous adhesive with the macro CTA (89.9%), surpassing that of the resilient hydrogel adhesive. Even after eight tensile cycles, the heterogeneous adhesive maintained a high resilience (>55%), whereas the resilience of the homogeneous adhesive sharply decreased to 25.5%.

We proposed that the reduced stress and improved resilience observed under increased strain might be due to two factors: a lower crosslinking density and continuous nanodomain structure (Figure 4d). First, the low crosslinking density of the adhesives resulted in a low modulus and a wide range of elastic deformations.[51] Second, better recovery and resilience resulted from strong connections within the hard domain. Previous studies have demonstrated that patterned adhesives with connected hard domains exhibit significantly better recovery properties than those with disconnected hard domains.[25]
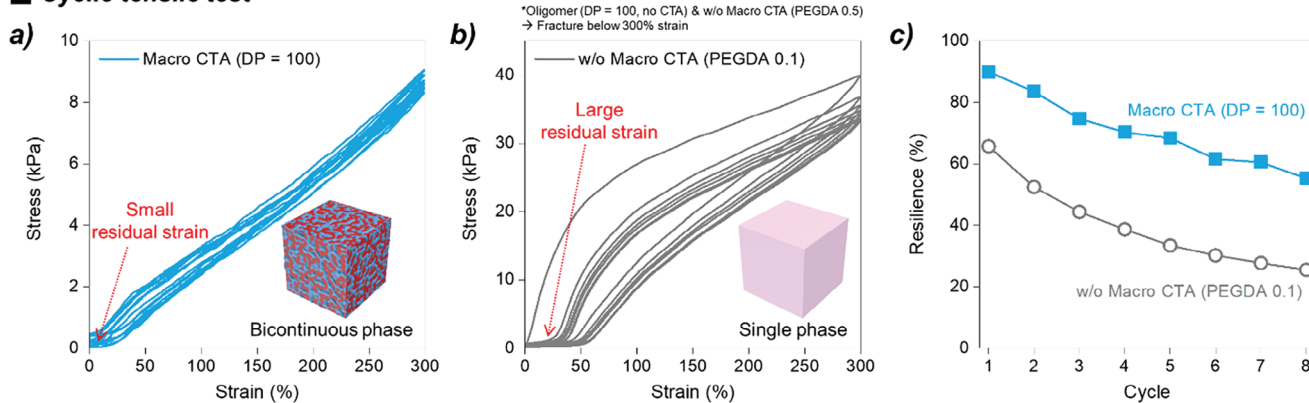
2.4. Adhesive Properties and Folding Stability

The adhesive properties of the prepared heterogeneous and homogenous adhesives were evaluated using peel-and-probe tack tests (**Figure 5**a,b). A shorter length of the PBA block in the macro CTA (DP = 80) resulted in a high probe tack but caused cohesive failure during the peel test owing to insufficient crosslinking density. Setting the DP of the macro CTA to 100 resulted in optimized peel strength (3.7 N/25 mm) and probe tack (5.7 N), comparable to common tapes such as scotch and masking tapes.[55] Moreover, the adhesion strength of the heterogeneous adhesive with the macro CTA (DP = 100) was significantly higher than that of the homogeneous (without macro CTA) and heterogeneous adhesives (with oligomer, no CTA, DP = 100). This improvement might be attributed to the appropriate crosslinking density rather than the bicontinuous nanodomain because adhesive strength is strongly linked to the crosslinking density of adhesive. Increasing the DP of the macro CTA resulted in a decrease in the peel strength and probe tack owing to the reduced wettability caused by the increased crosslinking density.

To confirm the excellent transparency offered by the nanoscale bicontinuous phase, UV/Vis spectra were used to assess the transparency of the prepared adhesives (Figure 5c). The adhesive film with a thickness of 60 μm exhibited high transparency regardless of the inclusion of the macro CTA. Additionally, the haze of the prepared adhesive was quantitatively evaluated to confirm that the heterogeneous adhesive exhibited no visible patterns that could be induced by differences in the refractive index between the soft and hard domains (Table S4, Supporting Information).

The heterogeneous adhesive with an optimized macro CTA (DP = 100) demonstrated high strain recovery, low modulus, and

ADVANCED
SCIENCE NEWS

www.advancedsciencenews.com

NANO · MICRO
small
www.small-journal.com

■ *Cyclic tensile test*

■ *Low modulus & high resilience of heterogeneous adhesive*
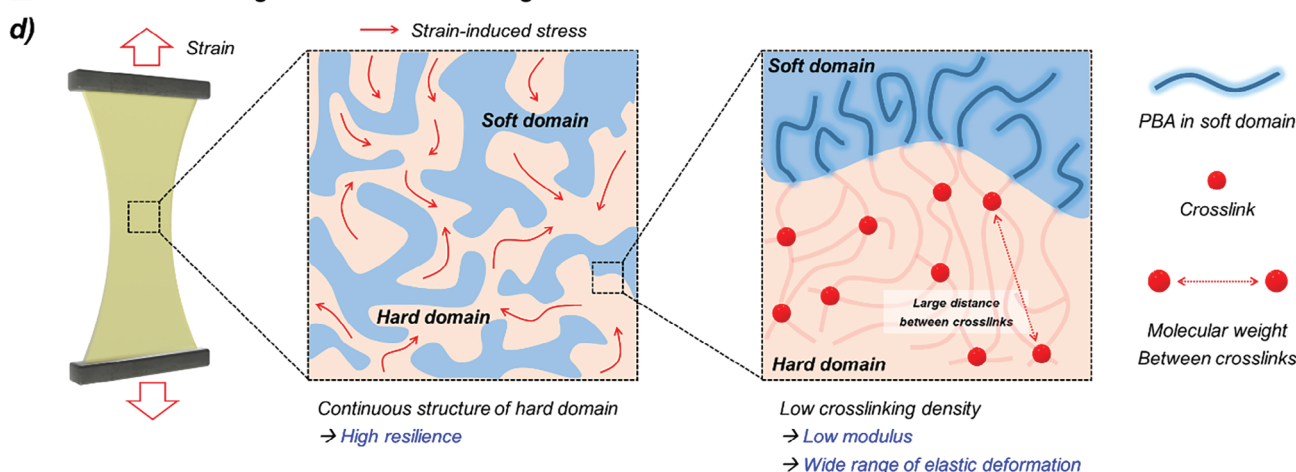

Figure 4. Cyclic tensile test results of the (a) heterogeneous (macro CTA, DP = 100) and (b) homogeneous adhesives (without macro CTA, PEGDA = 0.1). c) Dissipated energy per tensile cycle of the heterogeneous and homogeneous adhesives. d) Schematic illustration of low modulus and high resilience of the prepared heterogeneous adhesive.

sufficient adhesion strength. Therefore, a dynamic folding test was conducted to confirm the folding stability for use in foldable displays (Figure 5d). The test was conducted under three different conditions: 1) at room temperature (25 °C), 2) at low temperature (−20 °C), and 3) at high temperature combined with high humidity (60 °C & 93%RH) with varying numbers of folding cycles that are commonly used for assessing the folding stability of adhesives.[53] Notably, as shown in Figure 5e, the prepared heterogeneous adhesive exhibited excellent folding stability without any defects until the end of the folding cycle under all three conditions. In contrast, the homogeneous adhesive exhibited fractures under 25 and 60 °C and 93% RH. Even heterogeneous adhesives with the same overall monomer composition but with different DPs of the macro CTAs failed the folding test, except when the DP was 100 (Figure S6, Supporting Information). The exceptional folding stability of the optimized heterogeneous adhesive could be attributed to its unique structure, which included a bicontinuous nanodomain that offered high resilience and low stiffness. In summary, optimizing the length of the PBA block in the macro CTA resulted in a heterogeneous adhesive with superior stability to folding cycles, nearly satisfying the requirements for foldable electronics.

3. Conclusion

In this study, we developed innovative structured adhesives featuring nanoscale bicontinuous phases to produce flexible adhesives with low stiffness and high transparency. The formation of bicontinuous nanodomains was achieved via PIMS using a macro chain transfer agent (CTA). We observed phase separation, wherein the domain size increased by increasing the degree of polymerization (DP) of the macro CTA. This observation was confirmed using small-angle X-ray scattering, transmission electron microscopy, and dynamic mechanical analysis. The adhesive modulus exhibited a significant decrease with increasing DP of the macro CTA, owing to an increase in the crosslinking density. Despite the reduced modulus, the heterogeneous adhesives comprising soft and hard domains displayed excellent elasticity in both strain recovery and stress relaxation tests. Particularly, the optimized macro CTA length (DP = 100) yielded an adhesive with outstanding flexibility (strain recovery = 93%) and minimal modulus (maximum stress/applied strain = 7 kPa), thus surpassing conventional strategies. The optimized adhesive demonstrated high resilience (89.9%) even under extensive strain (300%), along with sufficient adhesion strength (peel strength:

■ *Adhesion property*
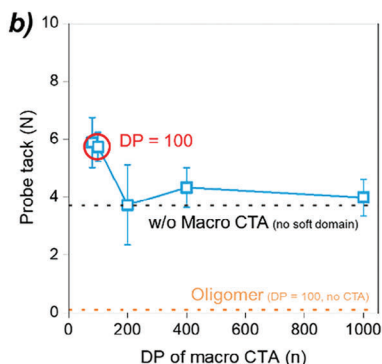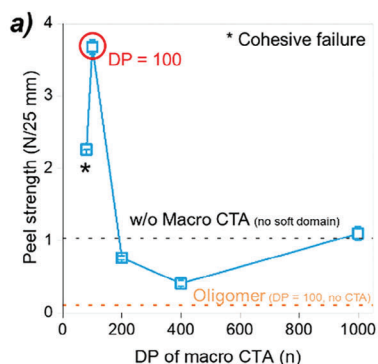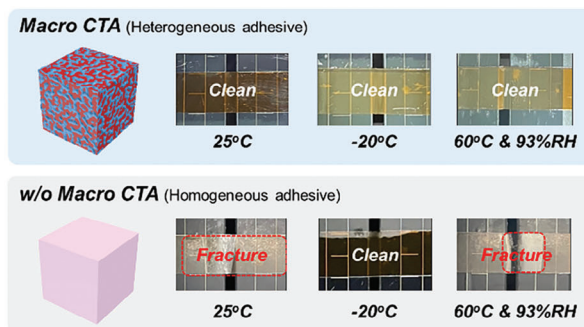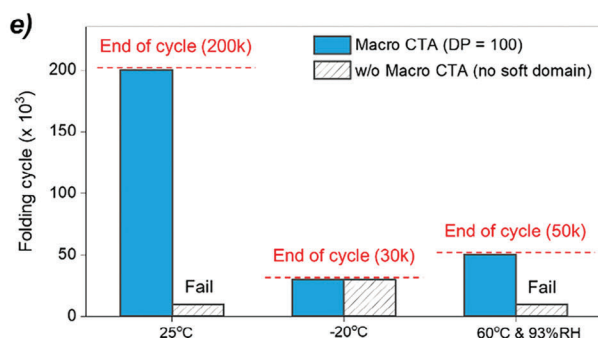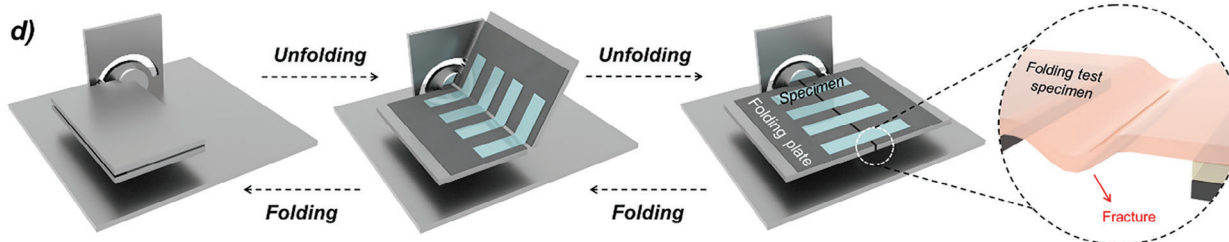

■ *Transparency*
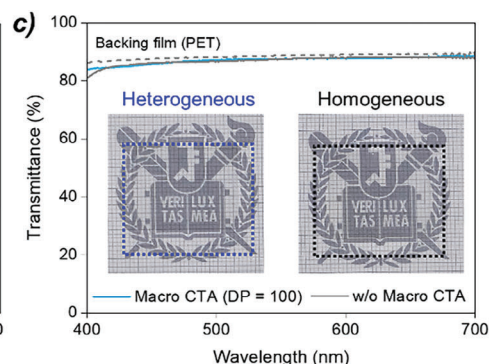
■ *Dynamic folding test*

Figure 5. a) Peel strength and (b) probe tack of the prepared adhesives with different DPs of the macro CTA. c) UV/Vis absorption spectra of the heterogeneous (macro CTA, DP = 100) and homogeneous (w/o macro CTA) adhesives. d) Schematic illustration of the dynamic folding test. e) Results of the dynamic folding test: folding cycle when failure occurred in the specimen. Images on the right show destroyed and normal specimens.

3.7 N/25 mm, probe tack: 5.7 N) and transparency. Moreover, dynamic folding tests revealed that the optimized heterogeneous adhesive exhibited exceptional folding stability over a wide range of temperatures and humidity levels. This excellent folding stability could be attributed to its unique structure, which was characterized by bicontinuous nanodomains with high resilience and low stiffness. In conclusion, the distinctive bicontinuous phase structure endowed the adhesive with excellent transparency and flexibility and reduced stiffness. These adhesive properties render it suitable for commercial foldable displays and suggest its potential applications in stretchable displays and wearable electronics.

Supporting Information

Supporting Information is available from the Wiley Online Library or from the author.

Conflict of Interest

The authors declare no conflict of interest.

Data Availability Statement

The data that support the findings of this study are available from the corresponding author upon reasonable request.

ADVANCED
SCIENCE NEWS

www.advancedsciencenews.com

NANO · MICRO

small

www.small-journal.com

[1] Y. Khan, A. Thielens, S. Muin, J. Ting, C. Baumbauer, A. C. Arias, *Adv. Mater.* **2020**, *32*, 1905279.

[2] W. Gao, H. Ota, D. Kiriya, K. Takei, A. Javey, *Acc. Chem. Res.* **2019**, *52*, 523.

[3] J. A. Rogers, T. Someya, Y. Huang, *Science* **2010**, *327*, 1603.

[4] T. R. Ray, J. Choi, A. J. Bandodkar, S. Krishnan, P. Gutruf, L. Tian, R. Ghaffari, J. A. Rogers, *Chem. Rev.* **2019**, *119*, 5461.

[5] Q. Han, C. Zhang, T. Guo, Y. Tian, W. Song, J. Lei, Q. Li, A. Wang, M. Zhang, S. Bai, X. Yan, *Adv. Mater.* **2023**, *35*, 2209606.

[6] P. Tan, H. Wang, F. Xiao, X. Lu, W. Shang, X. Deng, H. Song, Z. Xu, J. Cao, T. Gan, B. Wang, X. Zhou, *Nat. Commun.* **2022**, *13*, 358.

[7] D. Bryant, P. Greenwood, J. Troughton, M. Wijdekop, M. Carnie, M. Davies, K. Wojciechowski, H. J. Snaith, T. Watson, D. Worsley, *Adv. Mater.* **2014**, *26*, 7499.

[8] H. E. Lee, D. Lee, T.-I. Lee, J. H. Shin, G.-M. Choi, C. Kim, S. H. Lee, J. H. Lee, Y. H. Kim, S.-M. Kang, S. H. Park, I.-S. Kang, T.-S. Kim, B.-S. Bae, K. J. Lee, *Nano Energy* **2019**, *55*, 454.

[9] J. Park, Y. Lee, H. Lee, H. Ko, *ACS Nano* **2020**, *14*, 12.

[10] A. Carlson, S. Wang, P. Elvikis, P. M. Ferreira, Y. Huang, J. A. Rogers, *Adv. Funct. Mater.* **2012**, *22*, 4476.

[11] J. T. Abrahamson, H. Z. Beagi, F. Salmon, C. J. Campbell, in *Luminescence – OLED Technology and Applications*, IntechOpen, London, UK **2019**.

[12] E. Chang, D. Holguin, *J. Adhes.* **2005**, *81*, 495.

[13] W. C. Seok, J. T. Leem, H. J. Song, *Polym. Test.* **2022**, *108*, 107491.

[14] J. H. Lee, J. Park, M. H. Myung, M.-J. Baek, H.-S. Kim, D. W. Lee, *Chem. Eng. J.* **2021**, *406*, 126800.

[15] D. Lim, M.-J. Baek, H.-S. Kim, C. Baig, D. W. Lee, *Chem. Eng. J.* **2022**, *437*, 135390.

[16] C. J. Campbell, J. Clapper, R. E. Behling, B. Erdogan, H. Z. Beagi, J. T. Abrahamson, A. I. Everaerts, *SID Int. Symp. Dig. Tech. Pap.* **2017**, *48*, 2009.

[17] M. Nishimura, K. Takebayashi, M. Hishinuma, H. Yamaguchi, A. Murayama, *J. Soc. Inf. Display* **2019**, *27*, 480.

[18] F. Salmon, A. Everaerts, C. Campbell, B. Pennington, B. Erdogan-Haug, G. Caldwell, *SID Int. Symp. Dig. Tech. Pap.* **2017**, *48*, 938.

[19] G. F. Zapico, N. Takahara, K. Furuzono, R. Takahashi, F. Kawauchi, E. Ishikawa, T. Mansei, T. Makino, *SID Int. Symp. Dig. Tech. Pap.* **2021**, *52*, 1321.

[20] J.-H. Lee, T.-H. Lee, K.-S. Shim, J.-W. Park, H.-J. Kim, Y. Kim, S. Jung, *Int. J. Adhes. Adhes.* **2017**, *74*, 137.

[21] J.-H. Lee, G.-S. Shim, J.-W. Park, H.-J. Kim, Y. Kim, *J Ind Eng Chem* **2019**, *78*, 461.

[22] M.-B. Yi, T.-H. Lee, G.-Y. Han, H. Kim, H.-J. Kim, Y. Kim, H.-S. Ryou, D.-U. Jin, *ACS Appl Polym Mater* **2021**, *3*, 2678.

[23] M.-B. Yi, T.-H. Lee, S.-J. Lee, J.-S. Kim, H.-J. Kim, *Mater. Today Chem.* **2022**, *26*, 101141.

[24] J.-H. Back, D. Baek, K.-B. Sim, G.-Y. Oh, S.-W. Jang, H.-J. Kim, Y. Kim, *Ind. Eng. Chem. Res.* **2019**, *58*, 4331.

[25] J.-S. Kim, H.-J. Kim, Y.-D. Kim, *J. Mater. Res. Technol.* **2021**, *15*, 1408.

[26] F. d'Agosto, J. Rieger, M. Lansalot, *Angew. Chem., Int. Ed.* **2020**, *59*, 8368.

[27] N. J. Penfold, J. Yeow, C. Boyer, S. P. Armes, *ACS Macro Lett.* **2019**, *8*, 1029.

[28] M. J. Derry, L. A. Fielding, S. P. Armes, *Prog. Polym. Sci.* **2016**, *52*, 1.

[29] H. Moon, K. Jeong, M. J. Kwak, S. Q. Choi, S. G. Im, *ACS Appl. Mater. Interfaces* **2018**, *10*, 32668.

[30] J.-H. Back, Y. Kwon, J. C. Roldao, Y. Yu, H.-J. Kim, J. Gierschner, W. Lee, M. S. Kwon, *Green Chem.* **2020**, *22*, 8289.

[31] M. Zhu, Z. Cao, H. Zhou, Y. Xie, G. Li, N. Wang, Y. Liu, L. He, X. Qu, *RSC Adv.* **2020**, *10*, 10277.

[32] J.-H. Back, Y. Kwon, H.-J. Kim, Y. Yu, W. Lee, M. S. Kwon, *Molecules* **2021**, *26*, 385.

[33] J. Lequieu, A. J. Magenau, *Polym. Chem.* **2021**, *12*, 12.

[34] X. Mi, N. Liang, H. Xu, J. Wu, Y. Jiang, B. Nie, D. Zhang, *Prog. Mater. Sci.* **2022**, *130*, 100977.

[35] M. Seo, M. A. Hillmyer, *Science* **2012**, *336*, 1422.

[36] T. Oh, S. Cho, C. Yoo, W. Yeo, J. Oh, M. Seo, *Prog. Polym. Sci.* **2023**, *145*, 101738.

[37] K. Lee, N. Corrigan, C. Boyer, *Angew. Chem.* **2023**, *62*, 202307329.

[38] M. B. Larsen, J. D. Van Horn, F. Wu, M. A. Hillmyer, *Macromolecules* **2017**, *50*, 4363.

[39] D. Melodia, A. Bhadra, K. Lee, R. Kuchel, D. Kundu, N. Corrigan, C. Boyer, *Small* **2023**, 2206639.

[40] S. A. Chopade, S. So, M. A. Hillmyer, T. P. Lodge, *ACS Appl. Mater. Interfaces* **2016**, *8*, 6200.

[41] L. D. McIntosh, M. W. Schulze, M. T. Irwin, M. A. Hillmyer, T. P. Lodge, *Macromolecules* **2015**, *48*, 1418.

[42] M. W. Schulze, L. D. McIntosh, M. A. Hillmyer, T. P. Lodge, *Nano Lett.* **2014**, *14*, 122.

[43] X. Shi, V. A. Bobrin, Y. Yao, J. Zhang, N. Corrigan, C. Boyer, *Angew. Chem., Int. Ed.* **2022**, *61*, 202206272.

[44] V. A. Bobrin, K. Lee, J. Zhang, N. Corrigan, C. Boyer, *Adv. Mater.* **2022**, *34*, 2107643.

[45] V. A. Bobrin, Y. Yao, X. Shi, Y. Xiu, J. Zhang, N. Corrigan, C. Boyer, *Nat. Commun.* **2022**, *13*, 3577.

[46] D. Satas, *Handbook of Pressure Sensitive Adhesive Technology*, 3rd ed., Satas & Associates, Warwick, RI, USA **1999**.

[47] M. A. Droesbeke, R. Aksakal, A. Simula, J. M. Asua, F. E. Du Prez, *Prog. Polym. Sci.* **2021**, *117*, 101396.

[48] H. Jensen, J. H. Pedersen, J. J. Ørgensen, J. S. Pedersen, K. D. Joensen, S. B. Iversen, E. Øsgaard, *J. Exp. Nanosci.* **2006**, *1*, 355.

[49] G. Moad, *Polym. Int.* **2015**, *64*, 15.

[50] E. Hasa, J. P. Scholte, J. L. Jessop, J. W. Stansbury, C. A. Guymon, *Macromolecules* **2019**, *52*, 2975.

[51] I. A. Gula, H. A. Karimi-Varzaneh, C. Svaneborg, *Macromolecules* **2020**, *53*, 6907.

[52] K. R. Albanese, Y. Okayama, P. T. Morris, M. Gerst, R. Gupta, J. C. Speros, C. J. Hawker, C. Choi, J. R. de Alaniz, C. M. Bates, *ACS Macro Lett.* **2023**, *12*, 787.

[53] J. H. Back, Y. Kwon, H. Cho, H. Lee, D. Ahn, H. J. Kim, Y. Yu, Y. Kim, W. Lee, M. S. Kwon, *Adv. Mater.* **2023**, *35*, 2204776.

[54] G. Y. Han, J. Y. Park, J. H. Back, M. B. Yi, H. J. Kim, *Adv. Healthcare Mater.* **2024**, *13*, 2303342.

[55] J.-H. Back, C. Hwang, D. Baek, D. Kim, Y. Yu, W. Lee, H.-J. Kim, *Composites, Part B* **2021**, *222*, 109058.